

Thermodynamics of lanthanide and uranyl complexes with tetrahydrofuran-2,3,4,5-tetracarboxylic acid (THFTCA) †

Lester R. Morss,^a Kenneth L. Nash^{*a} and Dale D. Ensor^b

^a Chemistry Division, Argonne National Laboratory, Argonne, Illinois 60439, USA.

E-mail: nash@anlchm.chm.anl.gov

^b Department of Chemistry, Tennessee Technological University, Cookeville, TN 38505, USA

Received 18th August 1999, Accepted 13th December 1999

We present the results of an investigation of the thermochemistry of the complexation of La^{3+} , Nd^{3+} , Eu^{3+} , Dy^{3+} , Tm^{3+} , and UO_2^{2+} by tetrahydrofuran-2,3,4,5-tetracarboxylic acid (THFTCA). This predisposed structural analog to oxydiacetic acid (ODA) has been previously shown both to exhibit greater sensitivity to lanthanide cation radius than complexes with the unconstrained ODA and to form anomalously weak complexes with UO_2^{2+} . Our purpose is to interpret these observations in terms of the balance between enthalpy and entropy contributions to the overall complexation thermodynamics. Enthalpies have been calculated from titration calorimetry experiments both for the protonation of the free ligand and for the formation of selected 1:1 and 1:2 complexes in pH 2–3 acidic media ($I = 0.1 \text{ M}$). The complexation entropies for the lanthanide complexes have been calculated using the previously reported stability constants for the MH_2L^+ , MHL , and $\text{M}(\text{H}_2\text{L})^{2-}$. The stability constants for the uranyl complexes have been determined by potentiometric titration and these values used to calculate the thermodynamic parameters. Complexation enthalpies for the 1:1 lanthanide–THFTCA complexes (MH_2L^+ species) are nearly identical to those of the lanthanide ODA complexes. Therefore, the size-selectivity observed in the lanthanide–THFTCA complexes arises from the complexation entropy. The comparative weakness of the uranyl complexes with THFTCA also is accounted for thermodynamically in the entropy term. Calculations based on an electrostatic model for complexation entropy and molecular mechanics modeling are used to help interpret the experimental results.

Introduction

We have previously reported the stoichiometry and free energies of formation of lanthanide and uranyl complexes with the predisposed polycarboxylate ligand tetrahydrofuran-2,3,4,5-tetracarboxylic acid (THFTCA, also referred to as H_4L in the following).^{1–3} The opposite ends of the THF ring in THFTCA are identical to the non-constrained structural analogs oxydiacetic acid (ODA) and succinic acid respectively. THFTCA has been studied for its potential application to actinide and lanthanide separations and nuclear fuels processing. We also reported a design for a process to partition selectively uranyl from trivalent and tetravalent actinides using this reagent.³

Our previously reported stability constants indicate that the 1:1 complexes between THFTCA and trivalent lanthanide cations exhibit greater sensitivity to the size of cations than does the unconstrained analog ODA.^{1,2} We have likewise noted that the complexes formed between THFTCA and UO_2^{2+} are anomalously weak,³ accounting in large measure for the ability to accomplish the selective separation noted above. We surmised that each of these effects was likely related to the structural rigidity of the THFTCA ligand. The present investigation seeks to provide insight into relative contributions of enthalpy and entropy⁴ to the free energy of complex formation.

In the following, we report complexation enthalpies determined by titration calorimetry and calculated entropies for the reactions between La^{3+} , Nd^{3+} , Eu^{3+} , Dy^{3+} , Tb^{3+} , UO_2^{2+} and THFTCA. Our dual purpose is to examine the relationship between the observed effects and the structural rigidity of the

ligand, and to gain a greater understanding of the impact of ligand preorganization/predisposition on enthalpy–entropy compensation effects.

Experimental

Sample preparation

Aqueous ligand solutions were prepared gravimetrically using THFTCA (Tokyo-Kasai Ltd.) that had been dissolved in water, filtered to remove insoluble material, recrystallized by slow cooling of a hot saturated solution, and dried at room temperature. The recrystallized THFTCA was assayed by potentiometric titration as 99.4% based on the monohydrate $\text{C}_8\text{H}_8\text{O}_9 \cdot \text{H}_2\text{O}$. Potentiometric titrations were carried out at 25.0 °C. Lanthanide and uranyl stock solutions were prepared as described previously.^{2,5} Carefully recrystallized sodium perchlorate was used for control of the ionic strength (0.1 M). NaOH titrant solutions for potentiometry were prepared from 50% NaOH to minimize carbonate content and standardized by titration of primary standard potassium hydrogen phthalate. Analytical reagent grade HClO_4 was used to perform pH–p[H] calibration titrations.

Procedures

Titration calorimetry. Calorimetry experiments are conducted in our laboratory in a titration minicalorimeter of our own design and construction. It is comprised of a 60 ml gold-plated copper “minicalorimeter” vessel, a computer-controlled 1 ml buret (Radiometer, Inc., precision $\pm 0.0005 \text{ ml}$), and a Visual Basic program written at Argonne. The program measures and records the vessel and bath temperatures, sets and maintains the vessel at the desired experimental temperature using a current-controlled Peltier cooler, calibrates the instrument with precise injections of electrical energy, injects doses of

† Work performed under the auspices of the U.S. Department of Energy, Office of Basic Energy Sciences, Division of Chemical Sciences under contract number W-31-109-ENG-38.

titrant at desired intervals, and calculates calibration constants and enthalpies of each titration dose. The calorimeter vessel is in an air-jacketed submarine chamber maintained at 25.0 °C with temperature drift less than ± 0.0005 °C h⁻¹. It incorporates a pH probe (Orion Ross semimicro combination electrode) for on-line monitoring of solution pH. The minicalorimeter sensitivity is about 0.001 J.

In the free ligand titration experiments, the minicalorimeter was loaded with 50.0 ml of 0.0100 M Na₄L solution ($I = 0.1$ M, NaClO₄). The titrant was 0.250 M HClO₄. In the metal ion complexation experiments, the minicalorimeter vessel was loaded with 50.0 ml of either 0.00500 M Ln(ClO₄)₃ or 0.0100 M UO₂(ClO₄)₂ solution that had been adjusted to $I = 0.1$ M with NaClO₄ and $p[H] = 3.0$ with HClO₄. The titrant was 0.250 M H₄L for Ln³⁺ titrations and 0.500 M H₄L for UO₂²⁺ at an initial ionic strength of 0.1 M. The H₄L titrant solution was characterized prior to use by potentiometric titration. Dilution experiments were carried out with the same titrant into 0.1 M NaClO₄ at $p[H] = 3.0$. Observed reaction heats for metal complexation reactions were corrected for the heat of dilution of the respective titrants.

Potentiometry of uranyl-THFTCA complexes. In attempting to fit the calorimetric data, we observed that the stability constants we reported previously³ did not correlate adequately with the enthalpy titration data. Specifically, stability constants for the species UO₂(H₂L) were not determined in the earlier report. Therefore, we decided to redetermine the stability constants for the uranyl-THFTCA complexes adopting slightly modified experimental procedures from the previous experiments. A 250 ml stock solution of 0.002 M H₄L ($I = 0.1$ M, NaClO₄) was prepared and standardized by titration with freshly prepared NaOH titrant. Replicate samples of this standardized THFTCA solution were introduced into the potentiometric titration vessel and known amounts of UO₂(ClO₄)₂ were injected to M:L ratios of 1:1 and 1:2. Duplicate titrations were completed at each M:L ratio (the “duplicates” at 1:2 mole ratio differed in the total metal ion concentration by about 25%). The pH probe in all titrations was an Orion Ross semimicro combination electrode with 5.0 M NaCl as the reference electrolyte.

Results

The results of the potentiometric titrations of the uranyl-THFTCA mixtures are shown in Fig. 1. Though the titrations were carried out between $p[H]$ 2 and near neutral pH, the data were fit only up to $p[H]$ 5 to minimize the impact of the added uncertainties introduced by the hydrolysis of the uranyl cation or the complexes on the computed stability constants. The reported hydrolysis constants of UO₂²⁺ include a variety of polynuclear species.⁶ We included the following uranyl hydrolysis constants as fixed parameters in the fit procedure: UO₂OH⁺ ($\log \beta_{1-10} = -5.50$), (UO₂)₂(OH)₂²⁺ ($\log \beta_{2-20} = -5.89$) and (UO₂)₃(OH)₅⁺ ($\log \beta_{3-50} = -16.46$). The metal complex species found to give the best fit of the data from $p[H]$ 2.5 to 5.0 are UO₂H₂L, UO₂HL⁻, (UO₂)₂HL₂³⁻, and UO₂HL₂⁵⁻ with the respective stability constants (defined in terms of the equilibria: $m \text{ UO}_2^{2+} + h \text{ H}^+ + l \text{ L}^{4-} \rightleftharpoons (\text{UO}_2)_m \text{H}_h \text{L}_l^{2m+h-4l}$, β_{mhl}) $\log \beta_{121} = 14.27(\pm 0.05)$, $\log \beta_{111} = 11.18(\pm 0.02)$, $\log \beta_{212} = 20.30(\pm 0.06)$, and $\log \beta_{112} = 16.04(\pm 0.04)$ (uncertainties are at the $\pm 2 \sigma$ confidence interval). These constants produced the solid line fits shown in Fig. 1. The analysis of the data was accomplished using the program PSEQUAD.⁷

The spread of pK_a values of THFTCA is such that, except for the initial portion of the titration, there is significant overlap between the successive protonation reactions. Therefore, the dilution-corrected cumulative heats for the ligand protonation reactions are fit to the following function using a non-linear regression procedure:

Table 1 Thermodynamic properties for THFTCA protonation at 298 K and $I = 0.1$ M (NaClO₄)

Reaction	$\Delta G^a/\text{kJ mol}^{-1}$	$\Delta H^b/\text{kJ mol}^{-1}$	$\Delta S^c/\text{J mol}^{-1} \text{K}^{-1}$
$\text{H}^+ + \text{H}_3\text{L}^- \rightleftharpoons \text{H}_4\text{L}$	-9.9 ± 0.1	$+1.5 \pm 0.2$	$+38 \pm 1$
$\text{H}^+ + \text{H}_2\text{L}^{2-} \rightleftharpoons \text{H}_3\text{L}^-$	-18.0 ± 0.1	$+0.4 \pm 0.3$	$+62 \pm 1$
$\text{H}^+ + \text{HL}^{3-} \rightleftharpoons \text{H}_2\text{L}^{2-}$	-26.6 ± 0.2	$+1.3 \pm 0.3$	$+94 \pm 1$
$\text{H}^+ + \text{L}^{4-} \rightleftharpoons \text{HL}^{3-}$	-37.1 ± 0.4	-1.4 ± 0.6	$+120 \pm 2$

^a Ref. 2. ^b This research. ^c Calculated from $\Delta G = \Delta H - T\Delta S$.

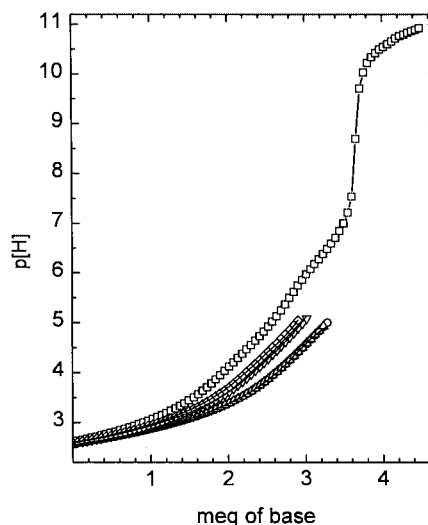


Fig. 1 Potentiometric titrations of \square 0.00198 M THFTCA with 0.0997 M NaOH; \circ , Δ 0.00198 M THFTCA, 0.00203 M UO₂(ClO₄)₂ with 0.0997 M NaOH; ∇ 0.00198 M THFTCA, 0.00101 M UO₂(ClO₄)₂ with 0.0977 M NaOH; \diamond 0.00198 M THFTCA, 0.000759 M UO₂(ClO₄)₂ with 0.0977 M NaOH.

$$\Sigma q_{\text{obs}} = m_{\text{HL}} \cdot \Delta H_{\text{HL}} + m_{\text{H}_2\text{L}} \cdot \Delta H_{\text{H}_2\text{L}} + m_{\text{H}_3\text{L}} \cdot \Delta H_{\text{H}_3\text{L}} + m_{\text{H}_4\text{L}} \cdot \Delta H_{\text{H}_4\text{L}} + m_{\text{H}} \cdot \Delta H_{\text{dil}} \quad (1)$$

where m_x refers to the number of moles of each species. The final term accounts for the excess free hydrogen ion whose dilution contributes to the heat at the end of the titration. The resolved protonation enthalpies and calculated entropies are shown in Table 1. The small ΔH values for the protonation reactions are consistent with the vast majority of published reports on the protonation heats of carboxylic acids.^{6,8}

In each of the titrations of free metal ion with THFTCA, we are introducing either 0.250 M or 0.500 M THFTCA (without any pH or ionic strength adjustment) into a solution either 0.005 M or 0.01 M in the metal ion in 0.001 M HClO₄ at $I = 0.1$ M. The calculated speciation of THFTCA in the respective titrants is (0.500 M THFTCA): $[\text{H}^+]_{\text{free}} = 0.0874$ M, $[\text{H}_4\text{L}] = 0.413$ M, $[\text{H}_3\text{L}^-] = 0.0860$ M, $[\text{H}_2\text{L}^{2-}] = 0.00068$ M and (0.250 M THFTCA): $[\text{H}^+]_{\text{free}} = 0.0596$ M, $[\text{H}_4\text{L}] = 0.191$ M, $[\text{H}_3\text{L}^-] = 0.0593$ M, $[\text{H}_2\text{L}^{2-}] = 0.00068$ M. The heat of dilution for each of the titrants was determined by titration into a solution 0.001 M HClO₄/0.099M NaClO₄. In the analysis of the metal complexation titrations, the experimental heats were corrected for this dilution heat and for the change in the degree of protonation of the uncomplexed ligand upon introduction into the calorimeter. We have chosen the species H₂L²⁻ as the base ligand to perform this correction. Reprotonation of the excess ligand (*i.e.*, that which does not react with metal ions) is also accounted for in attributing the heat of the complexation reaction. Cumulative heat sums Σq (corrected for dilution and ligand protonation) for complexation of THFTCA with Ln³⁺ or UO₂²⁺ are shown in Fig. 2, where a positive Σq refers to an endothermic effect. That these curves are non-linear is an

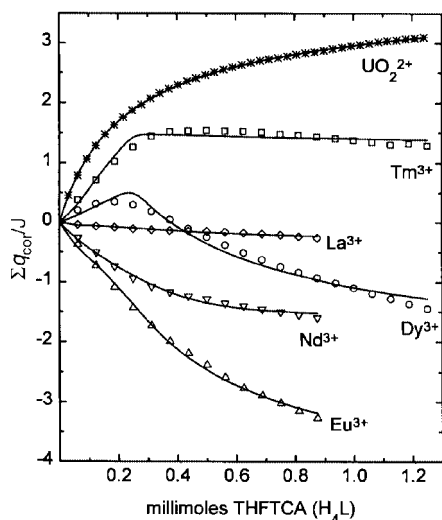


Fig. 2 Cumulative heats Σq (positive q is endothermic), corrected for heat of dilution and ligand protonation, in THFTCA titration calorimetry. For Ln^{3+} , titrant 0.25 M THFTCA–0.1 M NaClO_4 ; titrand 0.005 M $\text{Ln}(\text{ClO}_4)_3$ –0.1 M NaClO_4 . For UO_2^{2+} , titrant 0.50 M THFTCA–0.1 M NaClO_4 ; titrand 0.01 M $\text{UO}_2(\text{ClO}_4)_2$ –0.1 M NaClO_4 . Initial titrand volume 50.0 ml.

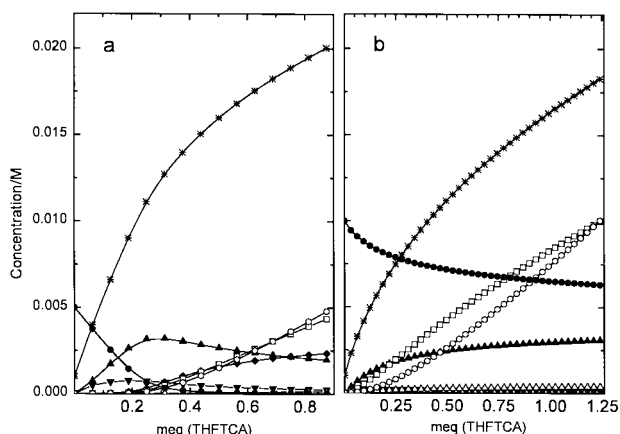
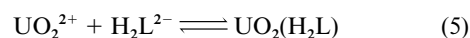
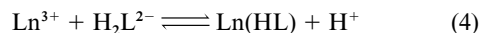
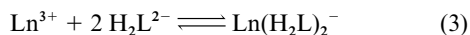
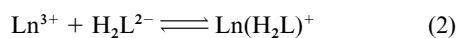


Fig. 3 Concentrations of important species during titration of (a) Eu^{3+} by THFTCA (H_4L). Titrant: 0.25 M THFTCA–0.1 M NaClO_4 . Titrand: 0.005 M $\text{Eu}(\text{ClO}_4)_3$ –0.1 M NaClO_4 ; volume 50.0 ml. (b) UO_2^{2+} by THFTCA (H_4L). Titrant: 0.50 M THFTCA–0.1 M NaClO_4 . Titrand: 0.01 M $\text{Eu}(\text{ClO}_4)_3$ –0.1 M NaClO_4 ; volume 50.0 ml. The species are \bullet (M_f), \blacktriangle (MH_2L), \blacktriangledown (MHL), \blacklozenge ($\text{M}(\text{H}_2\text{L})_2$), Δ (H_2L), \square (H_3L), \circ (H_4L), $*$ (H^+).

indication that each addition of titrant produces changes in more than one equilibrium.

The concentrations of metal complexes, free ligand species, and the equilibrium $\text{p}[\text{H}]$ were calculated using a Quickbasic program of our own design. The program uses as input the experimental conditions of the individual experiments and the appropriate equilibrium constants. Examples of the changes in species and $\text{p}[\text{H}]$ for Eu^{3+} and UO_2^{2+} during the titration are shown in Fig. 3. Solution $\text{p}[\text{H}]$ declines from 3.0 initially to a final value of 1.6–1.7. Calculated and experimentally measured pH agree adequately. The adjusted cumulative heats were correlated with changes in species concentrations and fit using the non-linear regression routines in Origin 4.0 (Microcal Software Inc., 1995). The solid lines shown in Fig. 2 represent the best fit adjustment of the unweighted data with the concentrations of the appropriate species for the individual (replicated) titrations.

Under the acidic conditions of these experiments, the equilibria accounting for the observed heats are as follows:



and



Based on the stability constants calculated herein, no higher order uranyl complexes (*i.e.*, $\text{M}:\text{L} = 1:2$) contribute under these conditions. Free hydrogen ion concentrations calculated by the program were used to calculate the concentrations of the complexed species.

In the La^{3+} , Nd^{3+} , Eu^{3+} , Dy^{3+} , and Tm^{3+} experiments, the enthalpies for the first 4–5 points represent overlapping contributions from reactions (2) and (4), predominantly (2). The subsequent 10–14 points in the titration are attributed to reaction (3). According to our previous potentiometric study, Tm^{3+} forms only 1:1 complexes with THFTCA, so the latter stage of that titration probably represents a simple dilution effect. In the uranyl experiments, the species $\text{UO}_2(\text{H}_2\text{L})$ is the dominant complex, with minor amounts of $\text{UO}_2(\text{HL})^-$ also present. The somewhat less satisfactory fit for the Tm^{3+} and Dy^{3+} data may indicate a minor contribution from an MH_hL_l complex that was not identified in the earlier potentiometric titrations. We have included this additional uncertainty in the calculation of error limits on the respective enthalpy and entropy data.

The Σq vs. $m(\text{THFTCA})$ plots are fit using a least squares regression routine fitting the model equation:

$$\Sigma q = \Delta H_{121} \cdot m_{\text{MH}_2\text{L}} + \Delta H_{111} \cdot m_{\text{MHL}} + \Delta H_{142} \cdot m_{\text{MH}_4\text{L}_2} \quad (7)$$

for the lanthanides and

$$\Sigma q = \Delta H_{111} \cdot m_{\text{MHL}} + \Delta H_{121} \cdot m_{\text{MH}_2\text{L}} \quad (8)$$

for uranyl. Subscripts on ΔH_{mhl} refer to the stoichiometry of the net complex $\text{M}_m\text{H}_h\text{L}_l$. The results of the fitting of the experimental data are shown in Table 2. Superficially, these results are typical in that complex stability for these highly ionic complexes is primarily entropy derived. It is also generally observed that the enthalpy of complexation of UO_2^{2+} is more endothermic than that for the lanthanide homologs.

Discussion

Lanthanide complexes

The samples of H_4L that we have studied have all been shown by X-ray crystallography to exist as the *trans-cis-trans* geometric isomer, which places the 2, 5 and 3, 4 carboxylate groups on opposite faces of the THF ring.² This isomer is also reported in the literature for the Cs^+ , Ca^{2+} , and tris(ethylenediamine)- $\text{Co}(\text{III})$ complexes with THFTCA.^{9,10} In this isomeric form, the ligand is unable to enter into a tetradentate coordination mode *via* the four carboxylates. The 2 and 5 carboxylates are arrayed at either side of the ether oxygen atom and hence are potentially capable of forming tridentate complexes with two five membered rings. The 3 and 4 carboxylates of THFTCA would form chelate complexes with one seven membered ring, typically considered a notably less stable geometry than a five or six membered chelate ring. The absence of free rotation around the C3–C4 bond will increase the stability of metal complexes formed at this site (relative to succinic acid). There is one report in the literature of a crystal structure for $\text{Ca}_2(\text{C}_8\text{H}_4\text{O}_9)(\text{H}_2\text{O})_6 \cdot 2\text{H}_2\text{O}$ in which Ca^{2+} ions are coordinated to THFTCA through both the 2, 5 carboxylates and the ether oxygen and through the 3, 4 carboxylates.⁹ However, Beitz has reported the displacement of three water molecules from the inner coordination

Table 2 Thermodynamic properties for Ln³⁺–THFTCA and UO₂²⁺–THFTCA complexation at 298 K and *I* = 0.1 M (NaClO₄)

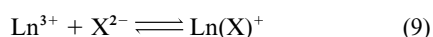
Reaction	M ⁿ⁺	Δ <i>G</i> /kJ mol ⁻¹	Δ <i>H</i> ^b /kJ mol ⁻¹	Δ <i>S</i> ^c /J mol ⁻¹ K ⁻¹
M ⁿ⁺ + HL ³⁻ ⇌ MHL	La ³⁺	-31.7 ± 0.9 ^a	ms ^d	ms ^d
	Nd ³⁺	-39.3 ± 1.0 ^a	-7.2 ± 7.0	+108 ± 24
	Eu ³⁺	-43.7 ± 0.8 ^a	-9.1 ± 4.2	+116 ± 14
	Dy ³⁺	-47.3 ± 0.2 ^a	ms ^d	ms ^d
	Tm ³⁺	-47.3 ± 0.2 ^a	+7.76 ± 4.10	+185 ± 14
	UO ₂ ²⁺	-26.7 ± 0.5	+22.5 ± 0.9	+166 ± 4
M ⁿ⁺ + H ₂ L ²⁻ ⇌ MH ₂ L	La ³⁺	-23.8 ± 0.4 ^a	+0.16 ± 0.59	+80 ± 3
	Nd ³⁺	-28.6 ± 0.9 ^a	-4.14 ± 1.44	+82 ± 6
	Eu ³⁺	-31.9 ± 0.5 ^a	-2.52 ± 1.16	+98 ± 4
	Dy ³⁺	-36.7 ± 0.2 ^a	+2.71 ± 0.48	+132 ± 2
	Tm ³⁺	-35.5 ± 0.2 ^a	+5.42 ± 0.72	+137 ± 3
	UO ₂ ²⁺	-17.8 ± 0.2	+18.2 ± 0.1	+121 ± 1
M ⁿ⁺ + 2 H ₂ L ²⁻ ⇌ M(H ₂ L) ₂	La ³⁺	-44.0 ± 0.7 ^a	-2.31 ± 0.48	+141 ± 6
	Nd ³⁺	-55.5 ± 1.5 ^a	-6.62 ± 0.40	+165 ± 6
	Eu ³⁺	-54.1 ± 0.7 ^a	-16.2 ± 0.8	+127 ± 5
	Dy ³⁺	-56.4 ± 0.5 ^a	-17.7 ± 1.3	+130 ± 6
	Tm ³⁺	—	—	—

^a Ref. 2. ^b This research. ^c Calculated from Δ*G* = Δ*H* - *T*Δ*S*. ^d ms = minor species. Uncertainties are ±2σ.

sphere of Eu³⁺ upon the addition of each of the first two H₂L²⁻ ligands¹¹ in aqueous solution. It is therefore likely that the lanthanide ions coordinate to THFTCA *via* the tridentate end of the molecule.

As noted above, the stability of lanthanide complexes with the unconstrained analog ligand ODA does not increase regularly across the lanthanide series. The log β₁₀₁ values for the Ln–ODA complexes increase from La–Sm, decrease between Eu and Tb, then slowly increase again from Dy–Lu.⁶ The mean log β₁₀₁ from Sm–Lu is 5.43(±0.14), a ±2.5% range in Δ*G* for a 15% change in cation radius.¹² This pattern is not unusual for lanthanide carboxylates and reflects contributions to the overall reaction from electrostatic attraction between the ligand and metal ion, a change in coordination number near Gd, and changes in hydration of the cations and complexes.

To compare thermodynamic data for lanthanide THFTCA and ODA complexes using species of the same formal charge, we focus on the 1 : 1 complexes between the lanthanide ions and the doubly protonated ligand species H₂L²⁻. The net reactions for comparing parameters is,



where X²⁻ is ODA²⁻ or H₂L²⁻. By focusing on species of formally like charges, we minimize the effect of gross electrostatic attraction on differences in complex stability.

The thermodynamic parameters relevant to reaction (9) for the two ligand systems are plotted in Fig. 4, where the closed symbols represent the THFTCA parameters and the open symbols describe the ODA system. The lower curves (Δ*G*) clearly illustrate that the free energy for Ln(H₂L)⁺ changes in a regular fashion from La to Dy and that the apparent size-selective effect disappears between Dy and Tm. It also demonstrates that the stability of the 1 : 1 lanthanide–ODA complexes does not vary monotonically across the series, as noted above. For the light lanthanides (La and Nd), the entropy contribution to Δ*G* is smaller (*i.e.*, less favorable) in the THFTCA system than in ODA, whereas for the heavy lanthanides the reverse is true. Complexation enthalpies for the two ligand systems are nearly identical across the series, suggesting that the net bond energies of the two ligands do not differ dramatically. In all systems, Δ*H* represents a minor contribution to Δ*G*, therefore overall complex stability is derived predominantly from the entropy term (*T*Δ*S*).

Uranyl complexes

For ligands to which the linear dioxo geometry of uranyl does not present a steric obstacle to complex formation, uranyl

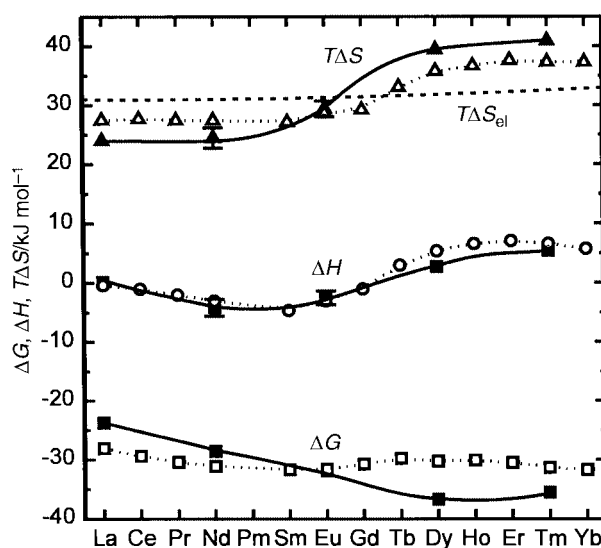


Fig. 4 Thermodynamic parameters for 1 : 1 lanthanide complexes with oxydiacetic acid (open symbols) and the diprotonated form of THFTCA (H₂L²⁻, closed symbols) according to the equilibrium Ln³⁺ + X²⁻ ⇌ LnX⁺. Dotted line represents electrostatic contribution to complexation entropy calculated using method in ref. 20.

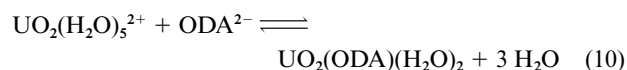
complexes are typically stronger than those of the trivalent lanthanides with the same ligand.¹³ For example, the 1 : 1 complexes between UO₂²⁺ and acetate are three times stronger than those of Eu³⁺ (log β₁₀₁(Eu) = 1.90 and log β₁₀₁(UO₂) = 2.44).⁶ We choose to compare these metal ions because crystal structures indicate that the metal–oxygen distances for both are about 2.39 Å (referring specifically to the equatorial coordination band for UO₂²⁺; the axial oxygens are more tightly bound at about 1.79 Å). In the corresponding malonate complexes, in which the bidentate malonate ligand can readily conform to the planar conformation demanded by UO₂²⁺, the uranyl complexes are nearly two orders of magnitude stronger (log β₁₀₁(Eu) = 3.72, log β₁₀₁(UO₂) = 5.42).⁶ For the ODA complexes, a potential steric mismatch in the UO₂²⁺ complex is suggested by the comparability of the europium and uranyl stability constants (log β₁₀₁(Eu) = 5.53, log β₁₀₁(UO₂) = 5.11).⁶

Reported crystal structures further indicate that the ether oxygen of ODA is more weakly bound by the UO₂²⁺ than the lanthanide cations. In Na₃[Ce(ODA)₃]·6H₂O, the carboxylate oxygen–Ce distances are 2.47 Å and the Ce–ether oxygen distance is 2.56 Å (a difference of 0.09 Å).¹⁴ In the nonahydrate, the corresponding distances are Ce–carboxylate oxygen 2.46–2.50 Å and Ce–ether oxygen, 2.59–2.60 Å, a difference of

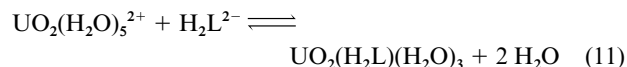
0.10–0.13 Å.¹⁵ In the hexahydrate of the Er complex, the Er–carboxylate oxygen distance is 2.33–2.36 Å, Er–ether oxygen 2.49–2.50 Å, a difference of about 0.14 Å.¹⁶ By comparison, the equatorial U–carboxylate oxygen distances are 2.43 Å and the U–ether oxygen distances are 2.63 Å in Na₂[UO₂(ODA)₂]·2H₂O, corresponding to a difference of 0.20 Å.¹⁷

For THFTCA, the tridentate face of the ligand appears to be further constrained from attaining a favorable arrangement of the donor atoms around the equatorial coordination zone of UO₂²⁺. The stability constant for formation of the complexes with the doubly charged ligand species H₂L²⁻ is log β₁₂₁ = 3.11 as compared with the value for the corresponding europium complex, log β₁₂₁(Eu) = 5.59. Though the Eu³⁺–THFTCA complex is comparable in stability to the Eu³⁺–ODA species, the uranyl–THFTCA complex is 10² weaker than the uranyl–ODA complex.

Thermodynamically, the weakness of the uranyl–THFTCA complex [as compared with UO₂(ODA)] is almost completely (about 85%) accounted for by a less favorable ΔS. The enthalpy for formation of UO₂(H₂L) (ΔH₁₂₁) is +18.2 kJ mol⁻¹ (for the reaction as formulated in equation (9)) as compared with +16.0 kJ mol⁻¹ for UO₂(ODA). This unfavorable complexation enthalpy is offset by the compensating entropies of ΔS_{UO₂H₂L} = +121 J mol⁻¹ K⁻¹ and ΔS_{UO₂ODA} = +153 J mol⁻¹ K⁻¹. The lower entropy for formation of the uranyl–THFTCA complex may indicate a net lower denticity for this complex (which allows the complex to retain more of the uranyl hydration sphere in the complex) than that in UO₂(ODA), as illustrated by the following equilibria:



and



The H₂L²⁻ ligand is almost certainly more strongly hydrated than ODA²⁻, but the comparability of the lanthanide ODA²⁻ and H₂L²⁻ entropies imply that this difference should not account for the uranyl observations.

Model comparisons

Christensen *et al.*⁸ have suggested an electrostatic model to explain the protonation thermodynamics of carboxylic acids, focusing mainly on mono- and di-carboxylic acids. Our results agree with the conclusions of Purdie *et al.*^{18,19} that such a correlation applies as well to aliphatic polybasic acids. It implies that the H⁺–O₂C–R interaction energy, as manifested by ΔH, is largely independent of the nature of R and the total number of carboxylates in the ligand. Examination of the literature suggests that this somewhat counterintuitive observation is unique to carboxylic acids. For phenols, amines, and polybasic inorganic acids (oxoacids), differences in the strength of binding of hydrogen ions are a function of both ΔH and ΔS for the protonation reaction.

As the interactions of lanthanide and actinide ions with chelating agents are predominantly electrostatic in nature, models based on Coulomb's law are often useful in explaining trends in experimental data. Manning²⁰ has developed a straight-forward model to permit calculation of the electrostatic contribution to the entropy (ΔS_{el}) associated with lanthanide binding to carboxylate-bearing ligands. The model is based on the difference in electrostatic interaction strength between a lanthanide cation, its coordinated water molecules, and the ligand functional groups. Deviations from the model may be attributable to second sphere hydration of the metal complex or to ligand structural features.

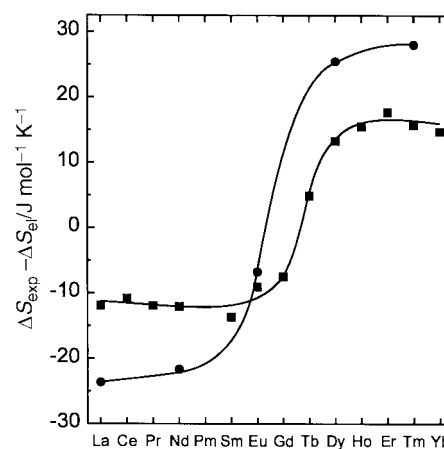


Fig. 5 “Non-electrostatic” contribution to complexation entropies for Ln(ODA)⁺ (■) and Ln(H₂L)⁺ (●).

The charge on the ligating groups, in the present case H₂O, R–CO₂⁻ and R–O–R, is calculated using the dipole moment of the “ligand” (we use the Manning value for the condensed dipole moment for H₂O of 2.68 D and the dipole moment for diethyl ether (μ = 1.15 D))[‡] and the metal–oxygen bond length. The formal charge of –1 is used for the carboxylate groups. The charge for each ligating group is used in a Born charging equation to calculate ΔS_{el} for the interaction of the metal ion with the functional group.

The individual entropies for the electrostatic interaction between the metal ion and the functional groups are summed to give the net entropy change associated with the one-for-one displacement of inner-sphere H₂O molecules by the ligand donor atoms. Applying this formula we calculate ΔS_{R–CO₂}(Eu) = +57.5 J mol⁻¹ K⁻¹, ΔS_{R–O–R}(Eu) = –9.7 J mol⁻¹ K⁻¹. The variation in lanthanide radii is such that these values increase slightly across the series, though the range is only about 3 J mol⁻¹ K⁻¹ per carboxylate and less than 1 J mol⁻¹ K⁻¹ for the ether.

The calculated ΔS_{el} for Eu-acetate (+57.5 J mol⁻¹ K⁻¹) and Eu-malonate (+115 J mol⁻¹ K⁻¹) are in surprisingly good agreement with the respective experimental values of +56 J mol⁻¹ K⁻¹ (I = 2.0 M) and +115 J mol⁻¹ K⁻¹ (I = 1.0 M),⁶ which suggests that the complexation entropies for these simple systems are consistent with this model. The model does not distinguish between ODA and THFTCA complexes of the lanthanides and produces the calculated value ΔS_{el} = 2ΔS_{R–CO₂}(Eu) + ΔS_{R–O–R}(Eu) = +105 J mol⁻¹ K⁻¹. From La³⁺ to Tm³⁺, ΔS_{el} ranges from +104 to +109 J mol⁻¹ K⁻¹.

In Fig. 5, we have plotted the non-electrostatic component of the experimental entropies (δ(ΔS) = ΔS_{exp} – ΔS_{el}) for the two ligand systems for the lanthanide complexes. The crossover from negative to positive deviations from the electrostatic model occurs near Tb³⁺ for the ODA complexes, but apparently near Gd for THFTCA. The light lanthanide complexes with ODA exhibit a constant entropy 12 J mol⁻¹ K⁻¹ lower (*i.e.*, less favorable for complex strength) than the electrostatic model while the heavy lanthanides average 16 J mol⁻¹ K⁻¹ higher. For the Ln(H₂L)⁺ complexes, the deviation is nearly twice as large both for the light and heavy lanthanide complexes. The crossover from lesser to greater entropy than the electrostatic prediction correlates more-or-less with the known change in average hydration number of the lanthanide aqua cations.²³ The magnitude of the difference between the light and heavy lanthanide ODA complexes is also roughly consistent with what

‡ The condensed dipole moment is the dipole moment of water in condensed media, as defined by Eisenberg and Kauzmann.²¹ The Manning value is within the range predicted by these authors. A more recent discussion of water dipole moments in condensed media can be found in ref. 22.

one might expect from the cratic entropy contribution from a water molecule released to the solution. We suggest that the increased deviation in the THFTCA complexes reflects a configurational contribution attributable to the structural rigidity of the ligand.

We have previously developed a linear free energy correlation between the strength of lanthanide complexes with oxygen donor ligands, the proton affinity of the ligand and the number of oxygen donor atoms available for metal ion binding.²⁴ Within this basic framework and in light of the apparent success of the electrostatic entropy calculation above, one might expect to observe a general correlation between thermodynamic parameters for metal complexation and the number of donor atoms available. We suggest that a hypothetical mixed-ligand complex between a lanthanide cation, acetate, and glycolate might exhibit the same net bonding strength as the corresponding ODA complex. This approach ignores ligand structural effects and possible differences in solvation of the free ligands and the complexes, but should to a first approximation not be adversely impacted by cratic entropy effects. It also assumes additivity of the 1:1 complexation thermodynamic parameters which would surely not be observed in an actual mixed ligand complex.

The thermodynamic parameters for Eu–acetate ($\Delta H_{EuAc} = +5.8 \text{ kJ mol}^{-1}$, $\Delta S_{EuAc} = +56 \text{ J mol}^{-1} \text{ K}^{-1}$, $I = 2.0 \text{ M}$) and Eu–glycolate ($\Delta H_{EuGly} = -3.0 \text{ kJ mol}^{-1}$, $\Delta S_{EuGly} = +37 \text{ J mol}^{-1} \text{ K}^{-1}$, $I = 2.0 \text{ M}$) when summed ($\Delta H_{sum} = +2.8 \text{ kJ mol}^{-1}$, $\Delta S_{sum} = +93 \text{ J mol}^{-1} \text{ K}^{-1}$) reproduce the corresponding Eu–ODA entropy surprisingly well but not the enthalpy ($\Delta H_{EuODA} = -3.0 \text{ kJ mol}^{-1}$, $\Delta S_{EuODA} = +94 \text{ J mol}^{-1} \text{ K}^{-1}$, $I = 1.0 \text{ M}$). The more exothermic ΔH_{EuODA} suggests increased strength for the interaction between Eu^{3+} and the ether oxygen in the tridentate chelate. A similar pattern is noted for the available thermodynamic data across the lanthanide series.

The simple sum of thermodynamic parameters for UO_2 –acetate and UO_2 –glycolate ($\Delta H_{\text{UO}_2\text{Ac}} = +11 \text{ kJ mol}^{-1}$, $\Delta S_{\text{UO}_2\text{Ac}} = +84 \text{ J mol}^{-1} \text{ K}^{-1}$, $\Delta H_{\text{UO}_2\text{Gly}} = +5.4 \text{ kJ mol}^{-1}$, $\Delta S_{\text{UO}_2\text{Gly}} = +64 \text{ J mol}^{-1} \text{ K}^{-1}$, $\Delta H_{sum} = +16.4 \text{ kJ mol}^{-1}$, $\Delta S_{sum} = +148 \text{ J mol}^{-1} \text{ K}^{-1}$, $I = 1.0 \text{ M}$) is very similar to the experimental data for UO_2 –ODA ($\Delta H_{\text{UO}_2\text{ODA}} = +16 \text{ kJ mol}^{-1}$, $\Delta S_{\text{UO}_2\text{ODA}} = +153 \text{ J mol}^{-1} \text{ K}^{-1}$, $I = 1.0 \text{ M}$). In contrast with the lanthanide calculations, the UO_2^{2+} data suggest that there is little net stabilization gained in this system due to coordination of the ether group. The relative elongation of the uranyl–ether oxygen bond noted in the crystal structure reports and the comparatively low values for $\Delta G_{\text{UO}_2\text{ODA}}$ (relative to the lanthanides) are consistent with this interpretation.

Finally, we have completed some simple molecular mechanics modeling calculations (ALCHEMY III, Tripos Associates, Inc., 1992) to examine the structural features of the uranyl and lanthanide complexes with THFTCA. The calculations indicate that whether UO_2^{2+} coordinates with THFTCA in the tridentate or bidentate (through the 3,4 carboxylates) modes, the -yl oxygens of the uranyl cation are brought into spatial conflict with some portion of the THFTCA ligand. In Fig. 6a, the uranyl is coordinated in a tridentate fashion to the 2 and 5 carboxylates and the ether oxygen. This coordination mode forces the THF ring into the position shown in which there may be a steric conflict between the -yl oxygens and the ring protons at the 3 and 4 positions. In the alternative bonding arrangement, shown as Fig. 6b, the spacing between the 3 and 4 carboxylates puts the -yl oxygens into conflict with the unbound oxygen atoms of the (3,4) carboxyl groups. The repulsion between these groups causes moderate torsional strain in the ligand, indicating a poor match between the metal ion and ligand structural features. Of the two configurations, the calculations indicate that there is substantially less ligand steric strain in the tridentate coordination mode. However, the comparative weakness of the complex (relative to the ODA analog) indicates that THFTCA is not bound strongly. By comparison, molecular mechanics

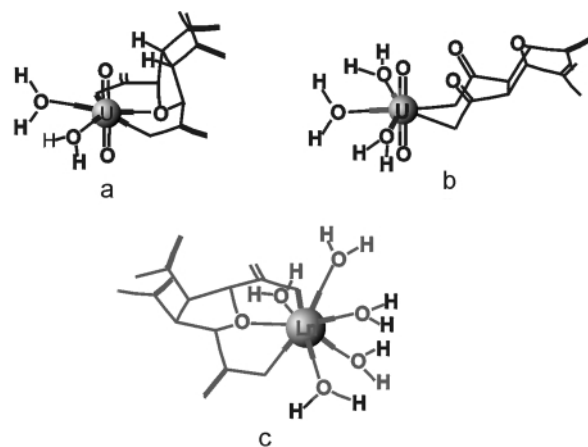


Fig. 6 Molecular mechanics (Alchemy III, Tripos Associates) calculated structures for proposed structures of UO_2^{2+} –THFTCA complexes, showing (a) UO_2^{2+} coordinated to the 2 and 5 carboxylates and the ether oxygen; (b) UO_2^{2+} coordinated to the 3 and 4 carboxylates; (c) Ln^{3+} in tridentate coordination mode.

calculations on the tridentate europium complex indicates almost no strain in the bound ligand (Fig. 6c).

Conclusion

Titration calorimetric results have established that the size-sensitivity demonstrated by THFTCA in its 1:1 complexes with lanthanide ions is a result of consistent changes in complexation entropy. The overall entropic stabilization of the complexes is consistent with an electrostatic model, though the electrostatic model does not account for the variation of complex stability across the lanthanide series. It appears likely that the correlations between complex stability and lanthanide atomic number is a result of differences in both inner sphere hydration and the configurational entropy of the bound THFTCA ligand.

Parallel studies of the thermodynamics of the reactions between UO_2^{2+} and THFTCA indicate that the complexes formed in this system are anomalously weak. The thermodynamic data and molecular mechanics modeling results suggest that the weakness is due to the incompatibility between the structural requirements of THFTCA and the linear dioxocation. Though the complexation enthalpies are similar for $\text{UO}_2(\text{H}_2\text{L})$ and $\text{UO}_2(\text{ODA})$, the entropies are $32 \text{ J mol}^{-1} \text{ K}^{-1}$ lower (less favorable) for the THFTCA complex. We interpret this result to indicate decreased dehydration of the uranyl cation occurs in the THFTCA complex than in the analogous ODA complex, probably attributable to lower denticity of the THFTCA ligand.

Acknowledgements

This work was sponsored by the Office of Basic Energy Sciences, Division of Chemical Sciences, U.S. Department of Energy under contract W-31-109-ENG-38. We thank Mark Jensen for numerous discussions, Paul Rickert for purification and characterization of the ligand, John Young for developing the titration calorimeter program, and John Hines for interfacing the Radiometer buret to the calorimeter.

References

- 1 K. L. Nash, *J. Alloys Compd.*, 1994, **213/214**, 300.
- 2 J. Feil-Jenkins, K. L. Nash and R. D. Rogers, *Inorg. Chim. Acta*, 1995, **236**, 67.
- 3 K. L. Nash, E. P. Horwitz, H. Diamond, P. G. Rickert, J. V. Muntean, M. D. Mendoza and G. di Giuseppe, *Solvent Extr. Ion Exch.*, 1996, **14**, 13.
- 4 E. Gallicchio, M. M. Kubo and R. M. Levy, *J. Am. Chem. Soc.*, 1998, **120**, 4526.

- 5 M. A. Hines, J. C. Sullivan and K. L. Nash, *Inorg. Chem.*, 1992, **32**, 375.
- 6 R. M. Smith, A. E. Martell and R. J. Motekaitis, *NIST Critical Stability Constants of Metals, Database 46, Version 2.0*, National Institute of Standards and Technology, Gaithersburg, MD, 1993.
- 7 L. Zekany and I. Nagypal, PSEQUAD: A Comprehensive Program for the Evaluation of Potentiometric and/or Spectrophotometric Equilibrium Data Using Analytical Derivatives, in *Computational Methods for the Determination of Formation Constants*, ed. D. J. Leggett, Plenum, New York, 1985, pp. 291–308.
- 8 J. J. Christensen, R. M. Izatt and L. D. Hansen, *J. Am. Chem. Soc.*, 1967, **89**, 213.
- 9 J. C. Barnes and J. D. Paton, *Acta Crystallogr., Sect. C*, 1984, **40**, 1809.
- 10 J. C. Barnes and J. D. Paton, *Acta Crystallogr., Sect. B*, 1982, **38**, 1588.
- 11 J. V. Beitz, Eu(III) interaction with water-soluble extractant: from speciation to photodestruction, in *Separations of f-Elements* (Proceeding of the Symposium on f Element Separations, 207th National Meeting of American Chemical Society, San Diego, California, 13–17 March 1994), ed. K. L. Nash and G. R. Choppin, Plenum, New York, 1995, p. 153.
- 12 R. D. Shannon, *Acta Crystallogr., Sect. A*, 1976, **32**, 751.
- 13 G. R. Choppin, *Radiochim. Acta*, 1983, **32**, 43.
- 14 J. Albertsson and I. Elding, *Acta Chem. Scand.*, 1977, **31**, 21.
- 15 I. Elding, *Acta Chem. Scand., Ser. A*, 1976, **30**, 649.
- 16 I. Elding, *Acta Chem. Scand., Ser. A*, 1977, **31**, 75.
- 17 G. Bombieri, F. Benetollo, A. D. Pra and R. Rojas, *J. Inorg. Nucl. Chem.*, 1973, **9**, 551.
- 18 N. Purdie, M. B. Tomson and N. Riemann *J. Solution Chem.*, 1972, **1**, 465.
- 19 N. Purdie and M. B. Tomson, *J. Solution Chem.*, 1972, **1**, 477.
- 20 T. J. Manning *J. Chem. Educ.*, 1996, **73**, 661.
- 21 D. Eisenberg and W. Kauzmann, *The Structure and Properties of Water*, Oxford University Press, New York, 1969.
- 22 J. K. Gregory, D. C. Clary, K. Liu, M. G. Brown and R. J. Saykally, *Science*, 1997, **275**, 814.
- 23 E. N. Rizkalla and G. R. Choppin, Lanthanides and Actinides Hydration and Hydrolysis, in *Handbook on the Physics and Chemistry of Rare Earths*, eds. K. A. Gschneidner, Jr., L. Eyring, G. R. Choppin and G. H. Lander, North Holland, Amsterdam, 1994, vol. 18, ch. 127, pp. 529–558.
- 24 K. L. Nash, *Eur. J. Solid State Inorg. Chem.*, 1991, **28**, 389.

Paper a906729i